ELSEVIER

Polymer 40 (1999) 695–700

polymer

Monte-Carlo simulation of polymers in shear flow

Sovirith Tan*

Laboratoire de Magnétisme des Surfaces, Université Paris 7- Denis Diderot, 2 Place Jussieu, 75251 Paris, France

Received 4 August 1997; revised 23 January 1998; accepted 3 March 1998

Abstract

The structural and dynamic properties of polymers, with excluded volume interactions, in simple shear flow, are investigated by a Monte-Carlo algorithm. Chain lengths of 5, 100 and 150 beads have been studied. For middle-sized polymers (100 or 150 beads), in strong shear, after the polymers have reached maximum elongation, beyond a shear rate threshold, the rear back of the polymer chains begins to fold and to spiral, in the wake of the running elongated polymer head. The potential part of the polymer's shear viscosity is evaluated at different shear rates, using non-equilibrium Monte-Carlo simulation. In spite of large statistical fluctuations of the shear viscosity computations, simulations for middle-sized polymers (100 or 150 beads) show a shear thinning behaviour. The simulation results should be compared with experiments.
© 1998 Elsevier Science Ltd. All rights reserved.

Keywords: Monte-Carlo simulation; Shear flow; Polymer viscosity

1. Introduction

Many extensive computer studies have been carried out on polymer problems, and various Monte-Carlo (MC) devices have been developed to generate efficiently macromolecular configurations [1]. There is no unique way to construct models of polymer systems, from lattice models to off-lattice models.

Many authors have studied kinetics of polymer chains with excluded volume on a lattice [2,3]. The 'slithering snake' model has been used to generate dynamic self-avoiding random chains on a lattice [4,5]. Some new schemes involving nonlocal move have been introduced [6–9]. In addition, the static properties of continuum, off-lattice and multichain systems have been investigated by a reptation Monte-Carlo algorithm [10].

Lai and Binder [11] have investigated grafted polymer layers under shear flow, using a Monte-Carlo (MC) simulation. Duering and Rabin [12] have reported Monte-Carlo (MC) simulation of polymers in shear flow near repulsive boundaries. Parnas and Cohen [13] have studied anchored polymer chains in simple shear flow, using Brownian dynamics simulation. Kremer and Grest [14] have used molecular dynamics and Brownian dynamics to investigate entangled polymer melt. This paper aims at investigating structural and rheological properties of polymers in homogeneous and unbounded shear flow, especially at very high shear rates.

2. Methods

2.1. Model and Monte-Carlo simulation

In order to investigate polymer shear flow, we have chosen the simplest off-lattice polymer model. Each polymer is modelled by a succession of $N = 5$, 100 and 150 spherical monomers, of radius $\sigma = 1$, jointed freely together by rigid bonds of length $l = 1$, at arbitrary angles. Monomers are free to move, subject to the rigid bonds constraint $l = 1$. Any pairs of monomers interact via a repulsive (shifted) Lennard–Jones hard potential, which takes account of the excluded volume in a convenient manner:

$$U(R) = \varepsilon.\left[\left(\frac{\sigma}{R}\right)^{12} - 2.\left(\frac{\sigma}{R}\right)^{6}\right] \quad R < \sigma$$
$$U(R) = 0 \qquad\qquad R > 0 \tag{1}$$

where R is the distance between monomers, and $\varepsilon = \sigma = 1$.

The steps of the Monte-Carlo procedure then consist of random rotations of bonds around the axis connecting the nearest neighbours beads along the chain, as indicated in Fig. 1.

The Metropolis algorithm is reported elsewhere [15,16]. I will recall the salient features. For each polymer chain, each

* Fax: +33 1 46 339401; E-mail: tan@ccr.jussieu.fr

0032-3861/98/$ - see front matter © 1998 Elsevier Science Ltd. All rights reserved
PII S0032-3861(98)00205-5

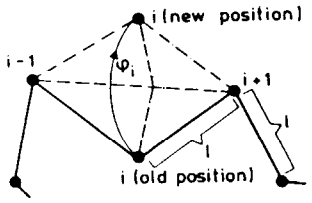

Fig. 1. Model of freely jointed chain: each polymer consists of N monomers, jointed together by rigid bonds of length l at arbitrary angles. The new position of a monomer i may be chosen by assigning an random angle ϕ_i from the interval [− 0.5 rad, + 0.5 rad].

bead is moved successively: bead 1,..., bead i,..., bead N. For example, bead i is rotated by an angle ϕ_i, selected randomly from the interval [+ 0.5 rad, − 0.5 rad], as described in Fig. 1. The bead interaction energy ΔE_i before and after the rotation are then compared. This virtual bead rotation is only carried out if the probability weight W_i = Min $\{\exp(-\Delta E_i/kT), 1\}$ exceeds a random number RAND distributed uniformly in the interval from zero to one. When thermal equilibrium is reached at a canonical temperature T, the Metropolis algorithm generates an ensemble of configurations distributed according to the Boltzmann weight.

The static and dynamic properties of such a simple model are trivial: the configurations of the chains for N large are Gaussian distributed, and their relaxation is described by the Rouse model [17,18]. This model is certainly a drastic oversimplification, which ignores chain connectivity and flexibility, and does not take account of the entanglement effects in polymer melts. However, this model is certainly fitted for non-equilibrium Monte-Carlo simulation. Via this model, the shear flow simulation is easily performed.

2.2. Simulation of shear flow

We have considered polymers of N = 5, 100 and 150 monomers, moving in homogeneous and unbounded flow. We have used periodic boundary conditions for polymers consisting of N = 5 monomers, and free boundaries for polymers consisting of N = 100 and 150 monomers.

A simple shear flow is introduced such that the velocity field is directed along the x-axis, and the gradient field along the y-axis:

$$v_x = \dot{\gamma}.y$$

where $\dot{\gamma}$ is the shear rate.

The MC step is chosen as an arbitrary unit of time $d\tau = 1$. During a small amount of time $d\tau$, the induced displacement of monomer i, located at (x_i, y_i, z_i) is

$$(\Delta x)_i = \dot{\gamma}.(y_i).d\tau \quad (2)$$

So, every 250 or 500 MC steps, we have chosen to update the position of each monomer i, and to add to its projection on the x-axis the flow-induced displacement $(\Delta x)_i$. This displacement is subject, of course, to the rigid bonds constraint l = 1, so the location of the nearest neighbour bead i + 1 along the y-axis and z-axis: y_{i+1} and z_{i+1}, must be corrected according to this constraint.

3. Result 1: Structural study of polymer configurations in shear flow

Polymer chains, consisting of N = 100 monomers, have been investigated, in the presence of simple shear flow, with different magnitudes of shear rates $\dot{\gamma}$, from $\dot{\gamma}$ = 1to $\dot{\gamma}$ = 24, at canonical temperature kT/ε = 0.8. Polymer chains, consisting of N = 150 monomers, have been considered, at shear rates $\dot{\gamma}$ in the interval [$\dot{\gamma}$ = 0.1, $\dot{\gamma}$ = 22], at temperature kT/ε = 1.5. Finally, polymer chains, consisting of N = 5 monomers, have been studied, at shear rates $\dot{\gamma}$ ranging from $\dot{\gamma}$ = 1 to $\dot{\gamma}$ = 24, at temperature kT/ε = 0.8.

Fig. 2 displays middle-sized polymer configurations (N = 100 or 150), at canonical temperatures kT/ε = 0.8 or 1.5, with a settled gradient velocity field $\dot{\gamma} = \frac{dV_x}{dy}$.

Already at shear rate $\dot{\gamma}$ = 0.1, shear flow effect is perceptible as regards random walk fluctuations of the chains, because of the unit scale of the shear rate fixed by choice of parameters in the MC simulation. At shear rate $\dot{\gamma}$ = 2 (Fig. 2a), shear flow effect cannot be neglected. At higher shear rate $\dot{\gamma}$ = 4 (Fig. 2b), all polymer chains (N = 150) are already stretched, but not still fully elongated in the shear flow x-axis. At shear rate $\dot{\gamma}$ = 6 (Fig. 2c), all polymer chains (N = 150) have reached their maximum elongation with respect to the flow direction x-axis.

At higher shear rate $\dot{\gamma}$ = 10 (Fig. 2d), the rear back of the polymer chains (N = 150), lingering behind in low velocity area ($y \approx 0$), begins to fold and to spiral, while the head of the polymer chains, located in higher velocity area, remains elongated. At shear rate $\dot{\gamma}$ = 12 (Fig. 2e), the spiralled curls spread out all over the polymer chains, like an hydrodynamic instability. At shear rate $\dot{\gamma}$ = 16 (Fig. 2f), the polymer chains are disentangled, and move forward towards each other.

All the successive polymer configuration sequences described above are condensed in Fig. 3, which displays the gyration radius R_g for polymer chains consisting of

Fig. 2. Middle-sized polymer configurations (N = 100 or N = 150 monomers), at temperatures kT/ε = 0.8 or 1.5, with a settled gradient velocity field $\dot{\gamma} = \frac{dv_x}{dy}$. (a) $\dot{\gamma}$ = 2, N = 100, kT/ε = 0.8. Some polymer chains can withstand shear flow. (b) $\dot{\gamma}$ = 4, N = 150, kT/ε = 1.5. Some polymer chains are stretched, but not still fully elongated in the shear flow x-axis. (c) $\dot{\gamma}$ = 6, N = 150, kT/ε = 1.5. All polymer chains have reached their maximum elongation with respect to the flow direction x-axis. (d) $\dot{\gamma}$ = 10, N = 150, kT/ε = 1.5. Some parts of the polymer chains begin to fold and spiral while heads of the polymer chains remain elongated. (e) $\dot{\gamma}$ = 12, N = 150, kT/ε = 1.5. The spiralling curls spread all over the polymer chains. (f) $\dot{\gamma}$ = 16, N = 150, kT/ε = 1.5. The polymer chains are disentangled and move forward towards each other.

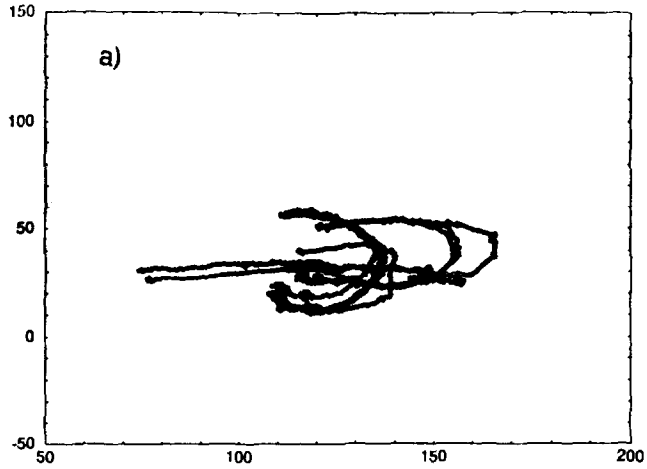
a)
150
100
50
0
-50
50
100
150
200

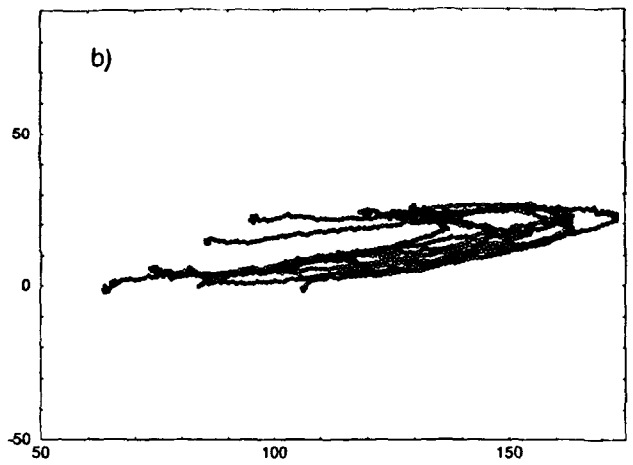
b)
50
0
-50
50
100
150

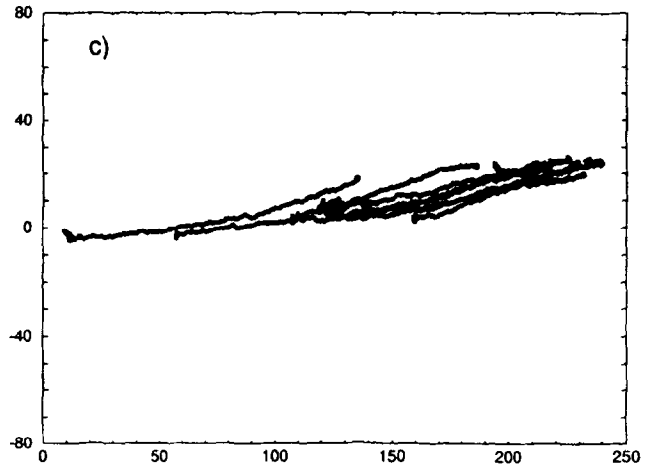
c)
80
40
0
-40
-80
0
50
100
150
200
250

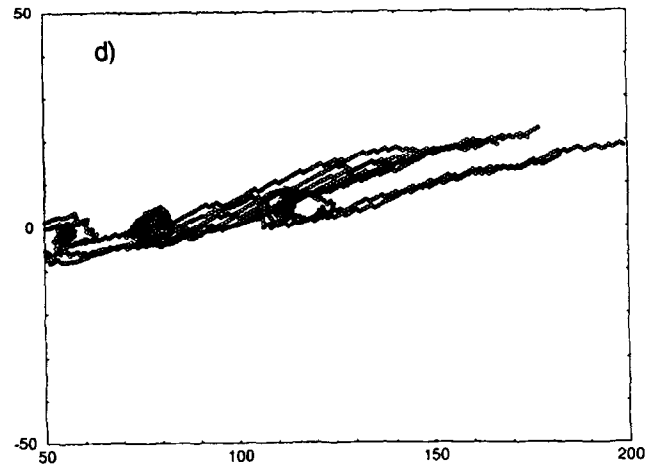
d)
50
0
-50
50
100
150
200

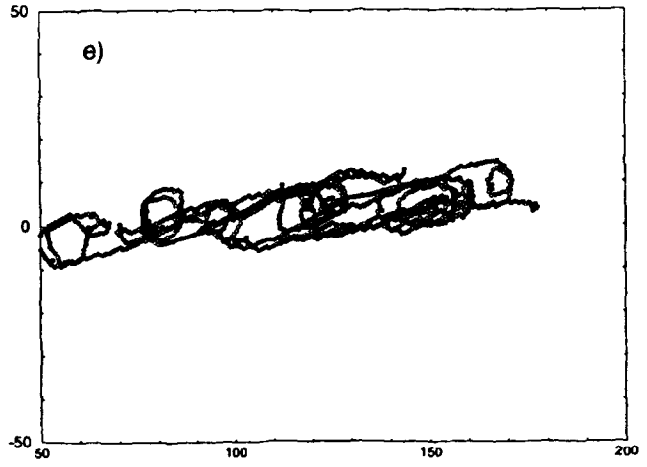
e)
50
0
-50
50
100
150
200

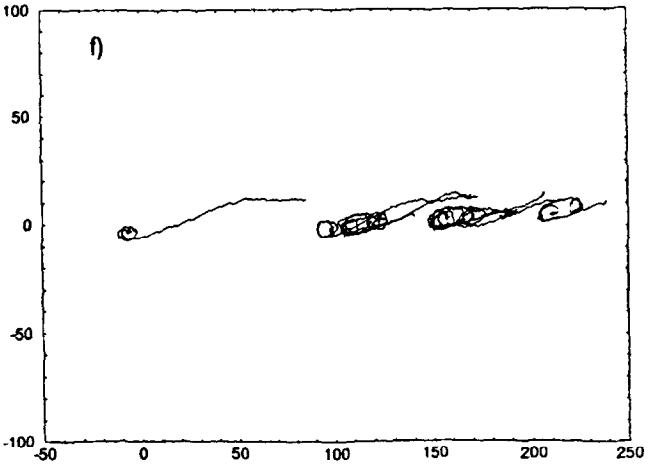
f)
100
50
0
-50
-100
-50
0
50
100
150
200
250

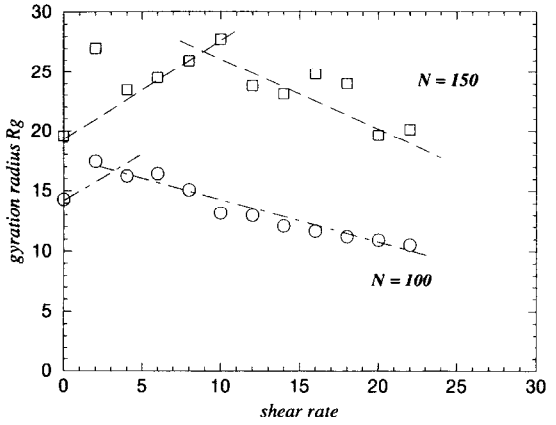

Fig. 3. Gyration radius R_g for polymer chains of $N = 150$ and $N = 100$ monomers. For $N = 150$ monomers, the polymer has reached its maximum elongation at shear rate $\dot{\gamma} \approx 8$. For $\dot{\gamma}$ ranging from $\dot{\gamma} = 0.1$ to $\dot{\gamma} = 10$, R_g increases, as the polymer chain starts to stretch. Beyond $\dot{\gamma} = 10$, R_g decreases, as the spiralling curl spreads along the chain. For $N = 100$ monomers, the polymer chain has already reached its maximum elongation at $\dot{\gamma} \approx 5$.

$N = 150$ and $N = 100$ monomers, each monomer located at (x_i, y_i, z_i):

$$R_g = \frac{1}{N}\left(\sum_{i=1}^{N}\left\{(x_i - x_{cm})^2 + (y_i - y_{cm})^2 + (z_i - z_{cm})^2\right\}^{1/2}\right) \quad (3)$$

where $[x_{cm}, y_{cm}, z_{cm}]$ is the position of the centre of mass.

For $N = 150$, the polymer chain has reached its maximum elongation at shear rate $\dot{\gamma} \approx 8$, and for $\dot{\gamma}$ ranging from $\dot{\gamma} = 0.1$ to $\dot{\gamma} = 10$, the gyration radius R_g increases regularly, as the polymer chain proceeds to stretch. Beyond $\dot{\gamma} = 10$, the gyration radius R_g decreases regularly, as the spiralling curl expands along the chain. For $N = 100$, the polymer chain has already reached its maximum elongation at shear rate $\dot{\gamma} \approx 5$.

Fig. 4 shows short-polymer chains configurations ($N = 5$ monomers) in shear flow at shear rate $\dot{\gamma} = 4$. At low shear rates ($\dot{\gamma} < 4$), short-polymer chains are elongated along the flow x-axis, as expected. However, at high shear rate, short-polymer chains are oriented at an angle $\theta = 45°$ with respect to the x-axis (or y-axis), as displayed in Fig. 4a. Moreover, short-polymer chains form layers, regularly stacked along the z-axis, as displayed in Fig. 4b, which is a projection of short-polymer chains on the plane $(x–z)$, and in Fig. 4c, which is a projection of short-polymer chains on the plane $(y–z)$.

3.1. Discussion

For polymer chains consisting of $N = 150$ and $N = 100$ monomers, stretching of the chain at increasing shear rate is expected, but what about the spiralling curl of the chain at high shear rate?

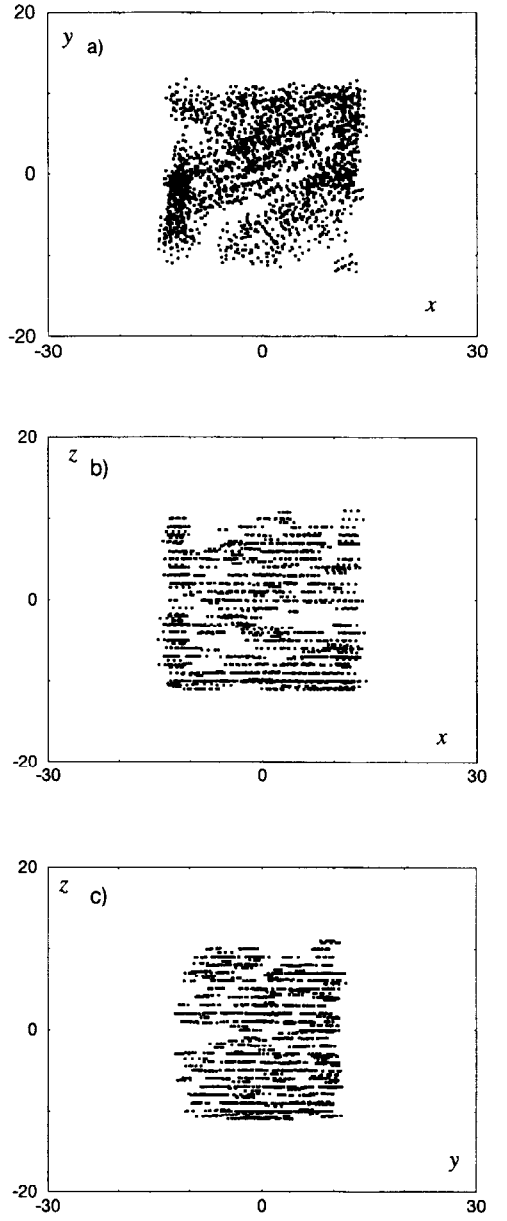

Fig. 4. Short-polymer chains configurations ($N = 5$ monomers) at temperature $kT/\varepsilon = 0.8$, with a settled gradient velocity field $\dot{\gamma} = 4$. (a) Projection on a $(x–y)$ plane. The short-polymer chains are oriented at an angle $\theta = 45°$ with respect to the x-axis (or y-axis). (b) Projection on a $(x–z)$ plane. The short-polymer chains form layers, regularly stacked along the z-axis. (c) Projection on a $(y–z)$ plane. The short-polymer chains form layers, regularly stacked along the z-axis.

If the velocity field gradient is very steep, the rear back of the polymer chain, located at lower velocity area, can no longer follow the head of the polymer chain, running at a higher velocity. Therefore, there is an accumulation of the monomers, lingering behind, in the wake of the running polymer head. To check the validity of these simulations, results should be compared with experiments.

To my knowledge, no report of such spiralling behaviour has been documented, although the simulation pictures (Fig.

2e and Fig. 2f) may show some structural resemblance to the lamellar order in Block Copolymer under shear flow, described in Ref. [19]. In fact, this behaviour may bear a closer analogy with the Rayleigh–Bénard hydrodynamic instability [20]: above a thermal gradient threshold, convection rolls appear in the liquid.

4. Result 2: Investigation of polymer's shear viscosity

The shear viscosity can be deduced from the long time behaviour of the equilibrium stress autocorrelation functions, which appear in the Green–Kubo transport formulae for viscosity. The shear viscosity consists of the so-called 'potential' component $\eta_{\phi\phi}$, the 'kinetic' component η_{KK}, and the 'cross' terms component $\eta_{K\phi}$ [21]:

$$\eta = \eta_{\phi\phi} + 2.\eta_{K\phi} + \eta_{KK} \tag{4}$$

where

$$\eta_{\phi\phi} = \lim_{t\to\infty}\beta\int_0^t \frac{1}{V}\langle J_\phi(0).J_\phi(u)\rangle du$$

$$\eta_{KK} = \lim_{t\to\infty}\beta\int_0^t \frac{1}{V}\langle J_K(0).J_K(u)\rangle du$$

$$\eta_{K\phi} = \lim_{t\to\infty}\beta\int_0^t \frac{1}{V}\langle J_K(0).J_\phi(u)\rangle du$$

where t is time, $b = 1/kT$, V is the volume. For a system of N monomers, each of mass m, with positions and velocities $\mathbf{r}_i$ and $\mathbf{v}_i$ and interacting pairwise through a potential $\phi(\mathbf{r}_i - \mathbf{r}_j)$, the stress tensors are:

$$J_\phi = -\frac{1}{2}\sum_{i\neq j}(r_{ij})_x.\left(\frac{\partial\phi(r_{ij})}{\partial r_{ij}}\right)_y \tag{5}$$

$$J_K = m.\sum(V_i)_x.(V_i)_y$$

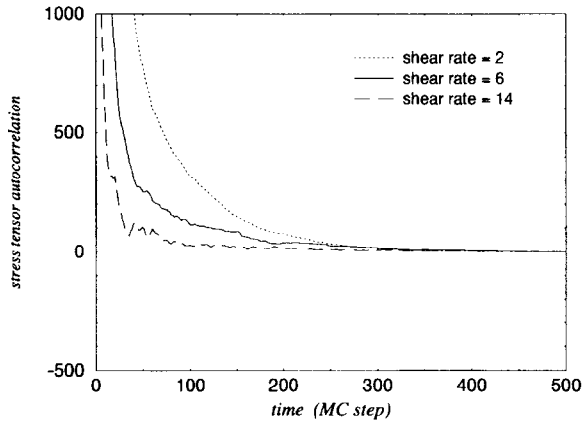

Fig. 5. Potential component of the stress tensor autocorrelation function, for short-polymer chains $N = 5$ monomers, at shear rates $\dot{\gamma} = 2$, 6 and 14.

The way via linear response theory and time correlation functions is subject to significant statistical error. The signal-to-noise ratio is particularly unfavourable at long times. Non-equilibrium Monte-Carlo simulations [21,22] may be used to improve the efficiency with which transport coefficients are calculated, and allow the signal-to-noise level of the measured response to be increased.

In addition, the potential component of the shear viscosity can be computed directly [21]:

$$\eta_{\phi\phi} = \frac{J_\phi}{\dot{\gamma}} \tag{6}$$

Fig. 5 shows the potential component $< J_\phi(0).J_\phi(t) >$ (t is time, here a MC step) of the stress tensor autocorrelation, for polymer chains $N = 5$ monomers, at shear rates $\dot{\gamma} = 2$, 6 and 14.

Fig. 6a displays the potential component of the shear viscosity $\eta_{\phi\phi}$ for polymer chains consisting of $N = 100$ monomers, at temperature $kT/\varepsilon = 0.8$. The potential part $\eta_{\phi\phi}$ of the shear viscosity is divided by a factor of 2 when the shear rate $\dot{\gamma}$ varies from $\dot{\gamma} = 2$ to $\dot{\gamma} = 22$.

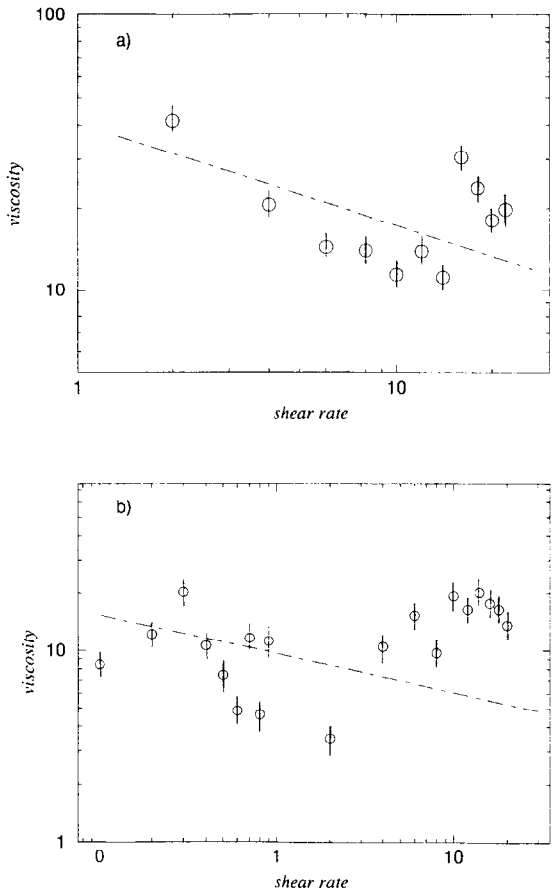

Fig. 6. Potential component of the shear viscosity for polymer chains of $N =$ 100 or $N = 150$ monomers, at temperature $kT/\varepsilon = 0.8$ or 1.5.(a) $N = 100$ monomers, $kT/\varepsilon = 0.8$ The potential part of the shear viscosity is divided by a factor of 2 when the shear rate $\dot{\gamma}$ varies from $\dot{\gamma} = 2$ to $\dot{\gamma} = 22$. (b) $N = 150$ monomers, $kT/\varepsilon = 1.5$. The potential component of the shear viscosity is divided by a factor of 2.5 when the shear rate $\dot{\gamma}$ varies from $\dot{\gamma} = 0.1$ to $\dot{\gamma} = 22$.

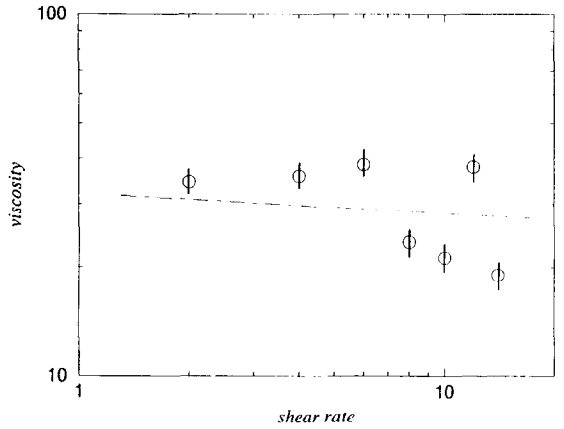

Fig. 7. Potential component of the shear viscosity, for polymer chains of $N=5$ monomers at temperature $kT/\varepsilon = 0.8$ The variation of the potential component of the shear viscosity is small (the viscosity is divided by a factor of 7/6 when the shear rate $\dot{\gamma}$ varies from $\dot{\gamma}=2$ to $\dot{\gamma}=14$).

Fig. 6b shows the potential component of the shear viscosity $\eta_{\phi\phi}$ for polymer chains consisting of $N = 150$ monomers, at temperature $kT/\varepsilon = 1.5$. The potential part $\eta_{\phi\phi}$ of the shear viscosity is divided by a factor of 2.5 when the shear rate $\dot{\gamma}$ varies from $\dot{\gamma}=0.1$ to $\dot{\gamma}=22$.

Finally, Fig. 7 displays the potential part of the shear viscosity $\eta_{\phi\phi}$ for polymer chains consisting of $N = 5$ monomers, at temperature $kT/\varepsilon = 0.8$. The variation of $\eta_{\phi\phi}$ of the shear viscosity is small (the variation factor is 7/6 when the shear rate $\dot{\gamma}$ varies from $\dot{\gamma}=2$ to $\dot{\gamma}=14$).

4.1. Discussion

The potential part $\gamma_{\phi\phi}$ of the shear viscosity for polymer chains of $N = 150$ and $N = 100$ monomers, is subject to large statistical fluctuations, because time correlation functions need an increased statistical effort, especially for large-sized polymer chains, which require long relaxation time. The correct reproduction of the dynamical behaviour requires long MC runs.

In spite of these statistical fluctuations, simulations of middle-sized polymer chains, with $N = 150$ and $N = 100$ monomers, show a trend towards shear thinning behaviour. This non-Newtonian behaviour [18] is less obvious for polymer chains of $N = 5$ monomers, whose potential part of the shear viscosity is almost constant in the range of shear rate $\dot{\gamma}$ simulated.

The experimental visco-elastic behaviour of polymer melts may be quite complex [18,23] . We do not expect a good agreement of our simulation results with experiments because the phantom chain model we used cannot give a fair account of the subtle interplay of intra- and inter-chains behaviour, such as entanglement effects.... However, we know that the Rouse model is not so bad, although this cannot be explained. We have also noticed that our normalized shear thinning slope is consistent with the experimental results of some copolymer melt (PA/P(MMA-CO-MAA) blends of polyamide with random copolymers of methyl methacrylate and methacrylic acid [24] and also data for the P-85 triblock copolymer of ethyline oxide (EO) and propylene oxyde (PO) [25]).

5. Conclusion

We have investigated the structural and rheological behaviour of polymer chains of $N = 5$, $N = 100$ and $N = 150$ monomers, in a homogeneous and unbounded shear flow, via non-equilibrium Monte-Carlo simulation. We have reported the unexpected behaviour of polymer chains at high shear rate, such as chains spiralling. A shear thinning behaviour for $N = 100$ and $N = 150$ monomers is also reported. All these simulation results should be compared with experiments.

References

[1] Binder K. Monte Carlo and molecular dynamics simulations in polymer science. Oxford: Oxford University Press, 1995.
[2] Verdier PH, Stockmayer WH. J Chem Phys 1962;36:227.
[3] Hilhorst HJ, Deutch JM. J Chem Phys 1975;63:5153.
[4] Wall FT, Mandel F. J Chem Phys 1975;63:4592.
[5] Wall FT, Chin JC, Mandel F. J Chem Phys 1977;66:3143.
[6] Lal M. Mol Phys 1969;17:57.
[7] MacDonald B, Jan N, Hunter DL, Steinitz MO. J Phys A: Math Gen 1985;18:2627.
[8] Madras N, Sokal AD. J Stat Phys 1988;50:109.
[9] Murat M, Witten TA. Macromolecules 1990;23:520.
[10] Bishop M, Ceperley D, Frisch HL, Kalos MH. J Chem Phys 1980;72:3228.
[11] Lai PY, Binder K. J Chem Phys 1993;98:2366.
[12] Duering E, Rabin Y. Macromolecules 1990;23:2232.
[13] Parnas RS, Cohen Y. Macromolecules 1991;24:4646.
[14] Kremer K, Grest GS. J Chem Phys 1990;92:5057.
[15] Tan S, Ghazali A, Lévy JCS. Surf Sci 1996;369:360.
[16] Tan S, Ghazali A, Lévy JCS. Surf Sci 1997;377-379: 997.
[17] Rouse PE Jr.. J Chem Phys 1953;21:1272.
[18] Ferry JD. Viscoelastic properties of polymers. New York: Wiley, 1980.
[19] Wang H, Kosani P, Barbara NP, Hammouda B. Macromolecules 1997;30:982.
[20] Manneville P. Dissipative structures and weak turbulence. New York: Academic Press, 1990.
[21] Erpenbeck JJ, Wood WW. J Stat Phys 1981;24:455.
[22] Naitoh T, Ono S. J Chem Phys 1979;70:4515.
[23] Engberg K, Ekblad M, Werner PE, Gedde UW. Polym Eng Sci 1994;34:1346.
[24] Degree R, Vanken R, Teyssié Ph. Polymer 1997;38:3861.
[25] Jorgensen EB, Hindt S, Brown W, Schillen K. Macromolecules 1997;30:2355.